Proceeding Paper

Self-Assembled Monolayers for Uricase Enzyme Absorption Immobilization on Screen-Printed Gold Electrodes Modified †

Héctor David Hernández [1], Rocio B. Dominguez [2] and Juan Manuel Gutiérrez [1,*]

1   Bioelectronics Section, Department of Electrical Engineering, CINVESTAV-IPN, Mexico City 07360, Mexico; hectord.hernandezm@cinvestav.mx
2   CONACyT-CIMAV S.C., Miguel de Cervantes 120, Complejo Industrial Chihuahua, CHIH, Chihuahua 31136, Mexico; rb.dominguezcruz@gmail.com
*   Correspondence: mgutierrez@cinvestav.mx; Tel.: +52-55-5747-3800
†   Presented at the 3rd International Electronic Conference on Biosensors, 8–21 May 2023; Available online: https://iecb2023.sciforum.net.

Abstract: Miniaturized and integrated devices for fast determination of clinical biomarkers are in high demand in the current healthcare environment. In this work, we present a functionalized self-assembled monolayer (SAM) on the gold surface of a screen-printed electrode (Au-SPE). The device was applied for uric acid (UA) detection, a biomarker associated with arthritis, diabetes mellitus, and kidney function. Prior to SAM formation, AuSPE was subjected to pretreatment with KOH and Au electrodeposition to provide additional roughness to the substrate. The SAM was formed in the AuSPE/KOH/AuNP surface by the cysteamine method—carried out for working surface dipping in the cysteamine (CYS) solution at 20 mM for 24 h (rinsed with ethanol and milli-Q water). Then, the uricase enzyme was immobilized through physical absorption at room temperature for 1 h to obtain the AuSPE/KOH/AuNPs/SAM/Uox biosensor. The physical and electrochemical characterization of AuSPE modification was carried out by scanning electron microscopy (SEM) and cyclic voltammetry (CV). The calibrated data of the Au/KOH/AuNPs/SAM/Uox biosensor showed a linear relation in the range of 50–1000 µM, a sensibility of 0.1449 µA/[(µM)cm^2], and a limit of detection (LOD) of 4.4669 µM. The Au/KOH/AuNPs/SAM/Uox also exhibited good selectivity for UA in the presence of ascorbic acid. Moreover, the methodology showed good reproducibility, stability, and sensitive detection of UA. This performance of the proposed biosensor is in good accordance with clinical needs and can be compared with previous biosensors based on nanostructured surfaces of high-fabrication complexity.

Keywords: AuNPs; AuSPE; biosensor; CV; electrochemist; uric acid; uricase; SAM

1. Introduction

Currently, electrochemical biosensors are indispensable tools for point of care applications (PoC) in medical monitoring and diagnostics due to their main advantages of easy miniaturizing, large response ranges, low limits of detection (LOD), high reproducibility, low costs, portability, etc. [1,2]. For biosensor development, screen-printed electrodes (SPE) are widely used [3] due to their simple design in electrochemical applications, allowing the implementation of tiny devices with high market availability at a low charge [4]. Some SPE advantages are high stability and sensibility in analytical application with a redox substance, disposable characteristics, good resistance to a variety of harsh electrolytes, mass production, and the availability of working electrodes modified with carbon or metallic inks such as silver and gold [5].

Although screen-printed gold electrodes (Au-SPE) have been less capitalized than their carbon counterpart, the Au-modified surface offers attractive advantages for protein binding through surface functionalization. One of the most effective techniques for surface modification is the use of thiol-based self-assembled monolayers (SAM), which are

spontaneously formed molecular assemblies over a solid substrate (such as Au-SPE) [6]. The SAM formation consists of the head groups or thiol groups (-SH) joining the Au working surface by chemisorption. On the other hand, the SAM structure is composed of aliphatic chains formed and ordered spontaneously during an incubation period [7]. For instance, Au-SPE with SAM formation has been demonstrated for immunosensors for [8–10]. However, biomolecules such as enzymes are equally prone to immobilization in such modified surfaces.

This work presents a simple enzymatic biosensor based on SAM produced over an AuSPE surface. The target analyte uric acid (UA) has relevance in multiple diseases, such as diabetes mellitus, kidney stones, and arthritis [11]. The UA electrochemical detection was performed through enzymatic action of the uricase enzyme (Uox), immobilized by physical absorption over the functionalized electrode. The developed biosensor showed a low limit of detection (LOD), good selectivity to ascorbic acid (AA) as an interfering analyte, and an extensive detection range that allows future clinical applications.

2. Materials and Methods

2.1. Reagents and Chemicals

All reagents were a chemical grade of the highest purity in accordance with The American Chemical Society. They were obtained from Sigma Aldrich, including potassium hydroxide (KOH), sulfuric acid (H_2SO_4), ethanol (C_2H_6O), potassium ferricyanide ($K_3[FeCN_6]$), chloroauric acid ($HAuCl_4$), cysteamine (C_2H_7NS), uric acid (C5H4N4O3), ascorbic acid (C6H8O6), uricase from Candida sp. (Uox-2 U/mg), bovine serum albumin (BSA), and hydrogen peroxide (H_2O_2) at 30%. A phosphate saline buffer (PBS) was prepared at 0.1 M and pH 7.4 with disodium phosphate (NaHPO4), monobasic phosphate (KH2PO4), sodium chloride (NaCl), and potassium chloride (KCl). Milli-Q water was used as the main dissolvent and for rinse processes.

2.2. Materials and Apparatus

The electrochemical characterization, the gold nanoparticle (AuNP) electrodeposition, and the UA detection were carried out using the Potentiostat 910 PSTAT mini (Metrohm, The Netherlands). AuSPEs (Metrohm, 6.1208.210) were used as working surfaces. All electrochemical assays were accomplished in a glass electrochemical cell. The physical characterization was performed by scanning electron microscopy (SEM) using the Hitachi SU3500 microscope (Tokyo, Japan).

2.3. Electrode Surface Modifications

The working surfaces were immersed for 10 min in a KOH solution at 50 mM and prepared in H_2O_2. This process eliminated superficial pollutants, mainly residual materials of the AuSPE manufacturing [12]. The AuNP electrodeposition on Au/KOH electrodes was carried out by cyclic voltammetry (CV) at 20 mV/s for two cycles from a potential of −0.5 V to +1 V, using $HAuCl_4$ at 1 mM dissolved in H_2SO_4 at 0.5 M [13]. For the SAM formation, the Au/KOH/AuNP electrodes were immersed for 24 h in a CYS solution at 20 mM prepared in an ethanol:water mixture of a 1:9 proportion [14]. Finally, 7 mg of Uox and 2 mg of BSA were dissolved in 200 μL of PBS for enzyme immobilization by physical absorption. Subsequently, 20 μL of this solution was placed on the Au/KOH/AuNPs/SAM working electrodes for 1 h at room temperature. The electrodes were rinsed to the end of each modification stage. The Au/KOH electrodes were rinsed with milli-Q water, the Au/KOH/AuNP and Au/KOH/AuNPs/SAM electrodes were rinsed with ethanol and milli-Q water, and for the last stage, the electrodes were rinsed with milli-Q water and PBS, obtaining the Au/KOH/AuNPs/SAM/Uox biosensor.

The general methodology of the working surface modification is shown in Figure 1.
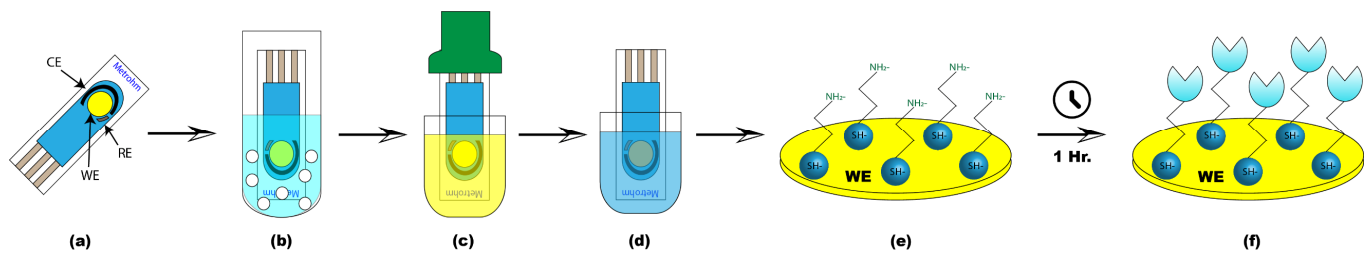
Figure 1. General methodology of the AuSPE surface modifications: (**a**) bare AuSPE (WE = Working electrode, CE = Counter electrode, and RE = Reference electrode), (**b**) G working surface activation with KOH/H_2O_2, (**c**) AuNP electrodeposition by CV with $HAuCl_4$, (**d**) SAM formation by CYS solution for 24 h of incubation, (**e**) SAM structure on working surface, and (**f**) complete assembly: Au/KOH/AuNPs/SAM/Uox biosensor.
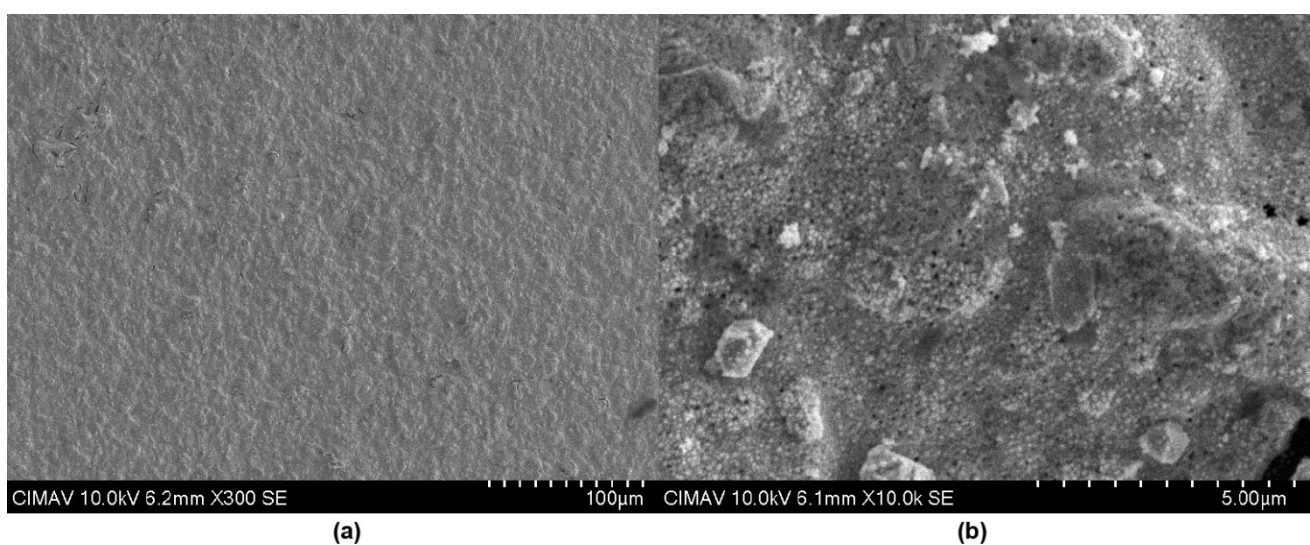
2.4. Electrochemical Assays

The electrochemical characterization was carried out for each surface modification stage by CV at 100 mV/s from a potential of -0.4 V to $+0.6$ V using a $K_3[FeCN_6]$ solution at 5 mM prepared in a KCl solution at 100 mM. UA solutions at 50 μM, 100 μM, 200 μM, 500 μM, and 1000 μM were prepared for analyte detection by CV at 100 mV/s from a potential of -0.3 V to $+0.8$ V using 100 mM PBS as a solvent.

The selectivity assay was carried out under the same conditions as the UA detection, using ascorbic acid (AA) at 1 mM as an interfering analyte.

3. Results and Discussion

3.1. Surface characterization

The SEM analysis verified the bare Au working electrode morphology before and after the AuNP electrodeposition. In Figure 2a, the view at ×300 shows the working surface as a continuous film with roughness and irregularities derived from the ceramic base on which the electrode is printed. In Figure 2b, the view at ×10,000 shows the AuNP distribution on the gold surface, which presented an average diameter of 22.53 nm. The AuNPs increased the molecular level interactions on the working surface due to their nanometric size, facilitating the -SH group interaction with the Au ions for the SAM formation [15].

Figure 2. *Cont.*

(c)
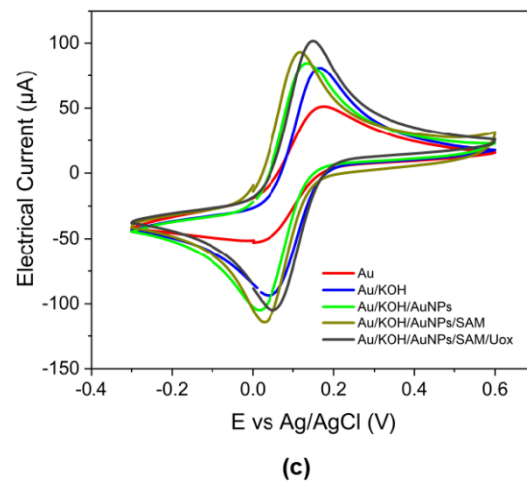
Figure 2. Working surface characterization: (**a**) view at ×300 of gold working electrode morphology, (**b**) view at ×10,000 of the gold working electrode with AuNPs electrodeposited, and (**c**) electrochemical characterization by CV in redox probe $K_3[FeCN_6]$/KCl at 5 mM for each working surface modification stage.

The electrochemical characterization of Figure 2c was carried out by CV, using the redox probe $K_3[FeCN_6]$/ KCl at 5 mM. The voltammograms showed that the redox reaction reversibility and the oxidation electrical current improved as the modification stages advanced, which indicates an enhanced electrochemical performance of the modified surface.

3.2. UA Detection by CV

The UA detection by CV was carried out with the Au/KOH/AuNPs/SAM/Uox biosensor using PBS. In Figure 3a, the voltammograms present an increased oxidation current when raising the UA concentration, while the oxidation potential was maintained around +0.5 V. Figure 3b presents the calibration curve through the linear regression of the current density depending on the UA concentration with R^2 = 0.9975. Based on the above, the Au/KOH/AuNPs/SAM/Uox biosensor presented a detection linear range of 50 μM to 1000 μM, with a sensitivity of 0.1449 μA/μM and a LOD (calculated as three times the standard deviation (σ) divided for sensitivity) of 4.4969 μM. Finally, Figure 3c presents the oxidation electrical current response of UA and AA (interfering analyte) at 1 mM (maximum measured concentration value). The voltammograms showed that due to the Uox selective action, the UA molecules' oxidation response was more significant than the AA molecules' oxidation response, exhibiting a selectivity of 85.1663%, with the enzymatic immobilization by the absorption method.

Table 1 presents a comparison of some similar devices aimed at UA detection in a PBS solution. The use of platinum–cobalt nanoparticles (bimetallic) offers a linear detection range fewer than the use of AuNPs, with an oxidation potential greater than that obtained with our device. On the other hand, the Nafion deposit on SPE provides a wide detection linear range. However, diseases associated with the UA biomarker tend to increase the serum concentration of this analyte, making a wider linear range desirable rather than ultra-low LOD.

For example, in blood serum, the UA levels are from 89 μM to 416 μM [16], which makes the proposed Au/KOH/AuNPs/SAM/Uox biosensor potentially suitable for a fast analysis of serum samples.
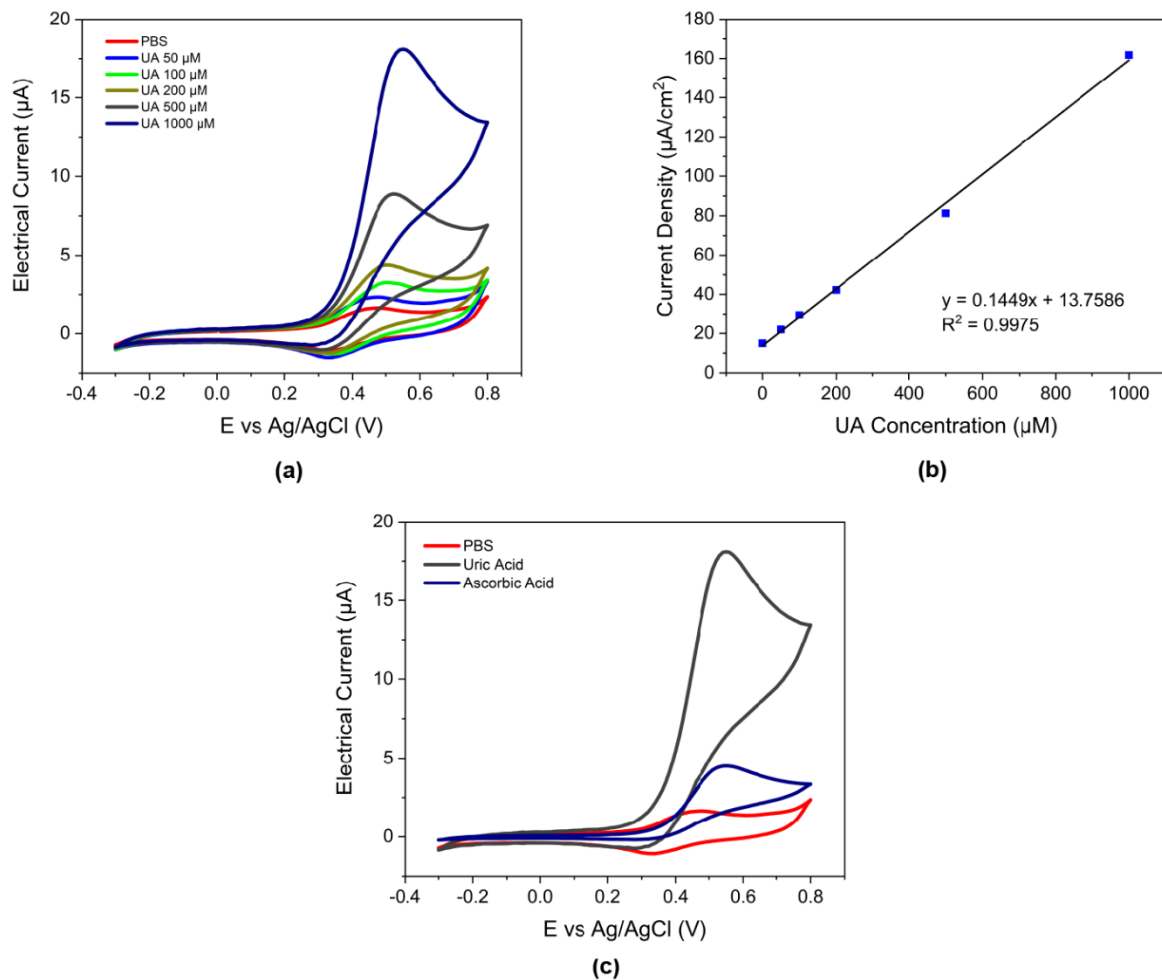
Figure 3. UA electrochemical detection: (**a**) UA detection by CV at different concentrations, (**b**) linear regression of the current density depending on the UA concentration, and (**c**) selectivity assay by CV in UA and AA solutions at 1 mM.

Table 1. General comparison with similar devices aimed at UA detection in PBS samples.

Surface	Linear Range (μM)	LOD (μM)	Potential (V)	Detection Technique	Reference
Pt-Co@rGO	5–800	0.1720	+0.65	CV & DPV	[17]
Nafion-SPCEs	62.5–5000	20.80	+0.3 to +0.5	DPV	[18]
GCE/Au-PDNs	40–200	0.0400	+0.4	CV & DPV	[19]
Au/KOH/AuNPs/SAM/Uox	50–1000	4.4969	+0.5	CV	This work

In this work, the Au/KOH/AuNPs/SAM/Uox biosensor repeatability was examined by developing many devices under the same conditions of fabrication, characterization, and UA detection. Our repeated measurements (n = 6) produced a notably low σ (<0.0129), reinforcing the fact that the electrochemical working areas remained with the same detection characteristics.

4. Conclusions

In this work, we present a simple biosensor development by exploiting the functionalization of AuSPE by SAM formation. The thiol-based SAM on AuSPE as a working surface was used for physical immobilization of Uox and subsequently in the detection of UA.

Surface modification was corroborated by SEM and CV, while UA detection was performed using CV in a range from 50 μM to 1000 μM. The device presented a good selectivity to UA against AA as an interfering analyte. The reported analytical results, as the detection linear range, sensitivity, and LOD, show our device as an attractive alternative for easy and fast UA monitoring.

References

1. Kampeera, J.; Pasakon, P.; Karuwan, C.; Arunrut, N.; Sappat, A.; Sirithammajak, S.; Dechokiattawan, N.; Sumranwanich, T.; Chaivisuthangkura, P.; Ounjai, P.; et al. Point-of-Care Rapid Detection of Vibrio Parahaemolyticus in Seafood Using Loop-Mediated Isothermal Amplification and Graphene-Based Screen-Printed Electrochemical Sensor. *Biosens. Bioelectron.* **2019**, *132*, 271–278. [CrossRef] [PubMed]
2. Reddy, K.K.; Bandal, H.; Satyanarayana, M.; Goud, K.Y.; Gobi, K.V.; Jayaramudu, T.; Amalraj, J.; Kim, H. Recent Trends in Electrochemical Sensors for Vital Biomedical Markers Using Hybrid Nanostructured Materials. *Adv. Sci.* **2020**, *7*, 1902980. [CrossRef] [PubMed]
3. Pérez-Fernández, B.; de la Escosura-Muñiz, A. Electrochemical Biosensors Based on Nanomaterials for Aflatoxins Detection: A Review (2015–2021). *Anal. Chim. Acta* **2022**, *1212*, 339658. [CrossRef] [PubMed]
4. Antuña-Jiménez, D.; González-García, M.B.; Hernández-Santos, D.; Fanjul-Bolado, P. Screen-Printed Electrodes Modified with Metal Nanoparticles for Small Molecule Sensing. *Biosensors* **2020**, *10*, 9. [CrossRef] [PubMed]
5. Pohanka, M. Screen Printed Electrodes in Biosensors and Bioassays. A Review. *Int. J. Electrochem. Sci.* **2020**, *15*, 11024–11035. [CrossRef]
6. Singh, M.; Kaur, N.; Comini, E. The Role of Self-Assembled Monolayers in Electronic Devices. *J. Mater. Chem. C* **2020**, *8*, 3938–3955. [CrossRef]
7. Love, J.C.; Estroff, L.A.; Kriebel, J.K.; Nuzzo, R.G.; Whitesides, G.M. Self-Assembled Monolayers of Thiolates on Metals as a Form of Nanotechnology. *Chem. Rev.* **2005**, *105*, 1103–1170. [CrossRef] [PubMed]
8. Martín-Fernández, B.; De-los-Santos-Álvarez, N.; Lobo-Castañón, M.J.; López-Ruiz, B. Hairpin-Based DNA Electrochemical Sensor for Selective Detection of a Repetitive and Structured Target Codifying a Gliadin Fragment. *Anal. Bioanal. Chem.* **2015**, *407*, 3481–3488. [CrossRef] [PubMed]
9. Nur Abdul Aziz, S.F.; Zawawi, R.; Alang Ahmad, S.A. An Electrochemical Sensing Platform for the Detection of Lead Ions Based on Dicarboxyl-Calix[4]Arene. *Electroanalysis* **2018**, *30*, 533–542. [CrossRef]
10. Pavithra, M.; Muruganand, S.; Parthiban, C. Development of Novel Paper Based Electrochemical Immunosensor with Self-Made Gold Nanoparticle Ink and Quinone Derivate for Highly Sensitive Carcinoembryonic Antigen. *Sens. Actuators B Chem.* **2018**, *257*, 496–503. [CrossRef]
11. Han, S.H.; Ha, Y.J.; Kang, E.H.; Shin, K.; Lee, Y.J.; Lee, G.J. Electrochemical Detection of Uric Acid in Undiluted Human Saliva Using Uricase Paper Integrated Electrodes. *Sci. Rep.* **2022**, *12*, 12033. [CrossRef] [PubMed]
12. Fischer, L.M.; Tenje, M.; Heiskanen, A.R.; Masuda, N.; Castillo, J.; Bentien, A.; Émneus, J.; Jakobsen, M.H.; Boisen, A. Gold Cleaning Methods for Electrochemical Detection Applications. *Microelectron. Eng.* **2009**, *86*, 1282–1285. [CrossRef]
13. El-Deab, M.S.; Okajima, T.; Ohsaka, T. Electrochemical Reduction of Oxygen on Gold Nanoparticle-Electrodeposited Glassy Carbon Electrodes. *J. Electrochem. Soc.* **2003**, *150*, A851. [CrossRef]
14. Leitao, C.; Pereira, S.O.; Alberto, N.; Lobry, M.; Loyez, M.; Costa, F.M.; Pinto, J.L.; Caucheteur, C.; Marques, C. Cortisol In-Fiber Ultrasensitive Plasmonic Immunosensing. *IEEE Sens. J.* **2021**, *21*, 3028–3034. [CrossRef]

15. Gabellini, C.; Şologan, M.; Pellizzoni, E.; Marson, D.; Daka, M.; Franchi, P.; Bignardi, L.; Franchi, S.; Posel, Z.; Baraldi, A.; et al. Spotting Local Environments in Self-Assembled Monolayer-Protected Gold Nanoparticles. *ACS Nano* **2022**, *16*, 20902–20914. [CrossRef] [PubMed]

16. Wang, Q.; Wen, X.; Kong, J. Recent Progress on Uric Acid Detection: A Review. *Crit. Rev. Anal. Chem.* **2020**, *50*, 359–375. [CrossRef] [PubMed]

17. Demirkan, B.; Bozkurt, S.; Şavk, A.; Cellat, K.; Gülbağca, F.; Nas, M.S.; Alma, M.H.; Sen, F. Composites of Bimetallic Platinum-Cobalt Alloy Nanoparticles and Reduced Graphene Oxide for Electrochemical Determination of Ascorbic Acid, Dopamine, and Uric Acid. *Sci. Rep.* **2019**, *9*, 12258. [CrossRef] [PubMed]

18. Xu, Z.; Zhang, M.-q.; Zou, H.-q.; Liu, J.-s.; Wang, D.-z.; Wang, J.; Wang, L.-d. Non-Enzymatic Electrochemical Detection of Uric Acid with Electrodeposited Nafion Film. *J. Electroanal. Chem.* **2019**, *841*, 129–134. [CrossRef]

19. Arroquia, A.; Acosta, I.; Armada, M.P.G. Self-Assembled Gold Decorated Polydopamine Nanospheres as Electrochemical Sensor for Simultaneous Determination of Ascorbic Acid, Dopamine, Uric Acid and Tryptophan. *Mater. Sci. Eng. C* **2020**, *109*, 110602. [CrossRef] [PubMed]